

For citation: Kuznetsova Z. A., Sinichenko M. I., Kuznetsov A. D., Kleshnina I. A., Sin'kovskiy F. K. Study of impeller design parameters effect on the axial thrust of a centrifugal electric pump assembly. *Siberian Journal of Science and Technology*. 2020, Vol. 21, No. 3, P. 389–399. Doi: 10.31772/2587-6066-2020-21-3-389-399

Для цитирования: Исследование влияния конструктивных параметров рабочего колеса на величину осевой нагрузки центробежного электронасосного агрегата / З. А. Кузнецова, М. И. Синиченко, А. Д. Кузнецов и др. // Сибирский журнал науки и технологий. 2020. Т. 21, № 3. С. 389–399. Doi: 10.31772/2587-6066-2020-21-3-389-399

STUDY OF IMPELLER DESIGN PARAMETERS EFFECT ON THE AXIAL THRUST OF A CENTRIFUGAL ELECTRIC PUMP ASSEMBLY

Z. A. Kuznetsova*, M. I. Sinichenko, A. D. Kuznetsov, I. A. Kleshnina, F. K. Sin'kovskiy

JSC Academician M. F. Reshetnev Information Satellite Systems
52, Lenin St., Zheleznogorsk, Krasnoyarsk region, 662972, Russian Federation

*E-mail: u-z-a@yandex.ru

This paper discusses and estimates the effect of some design parameters on the value of axial thrust appearing during functioning of the core component of a spacecraft's (SC) thermal control subsystem – electric pump unit (EPU). The major causes of axial forces in centrifugal pumps of in-line arrangement are described and analysed. Design parameters having an effect of axial thrust value are: impeller position relatively to EPU diffuser (position was chosen based on dimension chain calculation), presence and size of discharging holes in the impeller, number and shape of impeller vanes (numbers of 14 & 16 were considered). EPU impellers with different number and shape of vanes were designed and manufactured. A series of experiments was carried out in order to research the effects of all aforementioned parameters: measurements of head vs flow curves and axial thrust values at given flow values. Each parameter's contribution in the value of axial thrust appearing during EPU functioning is evaluated. Vibration measurements were obtained and analysed for electric motor DBE 63-25-6.3 fitted with different impellers. In this study, a DLP additive process was used for impellers manufacturing, which significantly sped up the tests. Obtained results will extend knowledge of processes taking place in EPU impellers, enable choice of the aforementioned parameters at design phase so to minimise axial thrust appearing during functioning of a centrifugal EPU of a spacecraft's thermal control subsystem. Outcomes of this study are capable of improving SC reliability at all phases of its life because EPU axial thrust causes its premature loss of operability.

Keywords: centrifugal pump, pump impeller, axial thrust, spacecraft thermal control subsystem.

ИССЛЕДОВАНИЕ ВЛИЯНИЯ КОНСТРУКТИВНЫХ ПАРАМЕТРОВ РАБОЧЕГО КОЛЕСА НА ВЕЛИЧИНУ ОСЕВОЙ НАГРУЗКИ ЦЕНТРОБЕЖНОГО ЭЛЕКТРОНАСОСНОГО АГРЕГАТА

З. А. Кузнецова*, М. И. Синиченко, А. Д. Кузнецов, И. А. Клешнина, Ф. К. Синьковский

АО «Информационные спутниковые системы» имени академика М. Ф. Решетнева»
Российская Федерация, 662972, г. Железногорск Красноярского края, ул. Ленина, 52

*E-mail: u-z-a@yandex.ru

В данной статье рассматривается и оценивается влияние некоторых конструктивных параметров на величину осевой нагрузки, возникающей при работе главного элемента активной жидкостной системы терморегулирования космического аппарата (КА) – электронасосного агрегата (ЭНА). Описаны и проанализированы основные причины возникновения осевой нагрузки в центробежном насосе с «осевым» принципом компоновки. Исследовались конструктивные параметры, влияющие на величину осевой нагрузки: положение рабочего колеса относительно диффузора ЭНА (положение выбиралось из расчета размерных цепей), наличие и размер разгрузочных отверстий в рабочем колесе, количество и форма лопастей рабочего колеса (рассмотрено количество лопастей 14 и 16). Были спроектированы и изготовлены рабочие колеса ЭНА с различным количеством и формами лопастей. Проведен ряд экспериментов по исследованию влияния всех перечисленных параметров: измерение расходно-напорных характеристик и величины осевой нагрузки при достижении определенного расхода. Дана оценка вклада каждого из перечисленных параметров на величину осевой нагрузки, возникающей при функционировании рабочего колеса. Была получена и проанализирована виброизмерительная информация на электродвигателе (ЭД) ДБЭ 63-25-6.3 с установленными поочередно рабочими колесами. В данном исследовании использовалась аддитивная технология печати DLP для изготовления рабочих колес, что значительно ускорило процесс испытаний. Полученные результаты способствуют расширению знаний о процессах, происходящих в рабочем колесе, позволяют осуществить выбор вышеперечисленных параметров на этапе проекти-

рования, способных снизить величину осевой нагрузки, возникающей при работе центробежного ЭНА в системе терморегулирования КА. Результаты данной работы способны повысить надежность функционирования КА во весь срок активного существования, поскольку повышенная осевая нагрузка в ЭНА является причиной его преждевременной потери работоспособности.

Ключевые слова: центробежный насос, рабочее колесо насоса, осевая нагрузка, система терморегулирования космического аппарата.

Introduction. Currently, there is a tendency for the appearance of Platforms with a thermal power of 8 to 10 kW on the world market of telecommunication spacecraft (SC) [1]. One of the possible options for structural design of the thermal control system (TCS) of such Platforms is a monophasic active TCS with a liquid coolant [2].

The most important element of this system is the electric pumping unit (EPU) [3], which provides continuous circulation of the coolant in the heat circuit, providing the thermal regime of the target and service equipment. Fail-safe operation of EPU during the entire active life of the spacecraft is a key indicator of the reliability of the entire spacecraft.

For the EPU of centrifugal type, reducing the axial thrust acting on the bearing arrangements of the pumps is one of the most important tasks of ensuring the long service life of the EPU.

This article presents the results of a study of the effect of the design parameters of the impeller of a single-stage centrifugal EPU on the axial thrust.

EPU design. The studied EPU refers to the “axial” principle of the layout: the main and standby centrifugal pumps are installed on the same axis, while the EPU housing is a single monoblock structure for both pumps, in which spiral diffusers for each pump are made in one piece [4]. In order to meet the high requirements for tightness, the pump motors are welded into the EPU housing through a bimetallic adapter. Fig. 1 shows a single-stage centrifugal EPU used in experiments in this study.

The technical parameters of such an EPU are presented in tab. 1.

Axial force in EPU. When the pump is started, an axial force of hydrodynamic origin, shown in fig. 1, begins to act on the bearing supports 3 (fig. 1) of the rotor 2.

The presence of this force affects the durability of the bearing supports 3 of the rotor of the electric motor 2 (fig. 1). This was confirmed in the course of studies of bearings that worked out during life tests in the electric motor of EPU. Inspection of the rotor bearings showed that they have numerous traces of wear in the form of dents, traces of friction, traces of metal transfer. In the course of metallographic research, it was found that these tracks are of a fatigue nature. According to the results of the study, it was found that the position of the wear marks on the rings indicates the presence of an axial thrust during the operation of the bearings. According to [5], the nature of the formation of axial force is the difference in pressure values in cavities “A” and “B” between the impeller and the casing. The area of the outer surface of the main disc under the discharge pressure is larger than that of the cover disc, which results in a static pressure force directed towards the inlet funnel. Fig. 2 shows the direction of action of forces in the EPU impeller. In this case, the difference between F_A and F_B is always directed towards the flow entering the impeller, and it is applied to the impeller, and through it to the bearing supports of the pump rotor. Thus, based on the nature of the formation of the axial force, it follows that to reduce it, it is necessary to eliminate the difference between F_A and F_B .

The geometric parameters of the impeller of the studied EPU are shown in fig. 3.

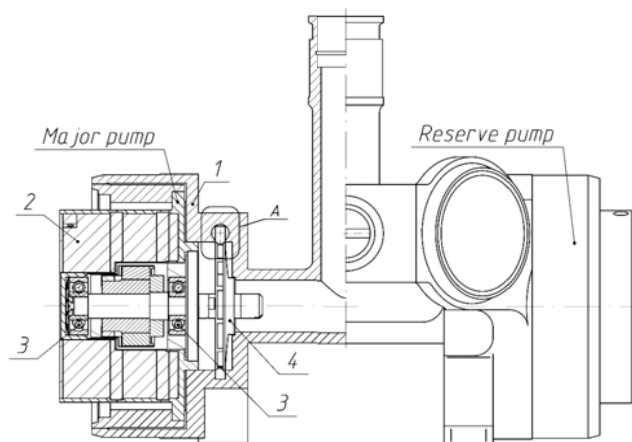


Fig. 1. Single-stage centrifugal electric pump unit:
1 – electric pump unit housing; 2 – motor; 3 – journal bearing; 4 – impeller

Рис. 1. Одноступенчатый центробежный ЭНА:
1 – корпус ЭНА; 2 – электродвигатель; 3 – радиальные подшипники; 4 – рабочее колесо

Technical parameters of EPU with standard impeller

Parameter name	Parameter value
Head (ΔP), kgf/cm ²	0.61
Flow rate (Q), m ³ /s	110–150
Rotational speed of the electric motor (n), rpm	5800
Power fluid	LZ-TK-2
Axial thrust, N	> 9.8

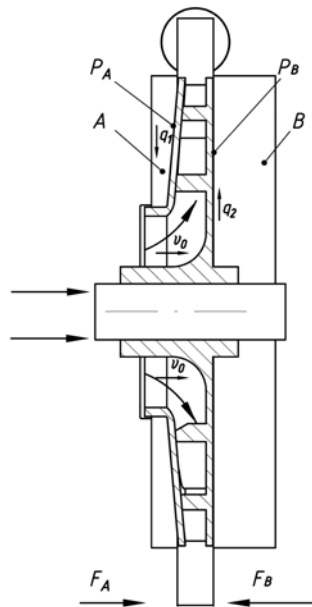


Fig. 2. The direction of the forces in the pump rotor:

A, B – pressured cavities; P_A – rotor top disk area;
 P_B – disk with blades area; F_A – axial force acting from the top disk;
 F_B – axial force acting from the disk with blades

Рис. 2. Направление действия сил на рабочее колесо ЭНА:
 A, B – полости, где действует давление; P_A – площадь покрывного
 диска рабочего колеса; P_B – площадь диска с лопатками;
 F_A – осевая сила, действующая со стороны покрывного диска;
 F_B – осевая сила, действующая со стороны основного диска

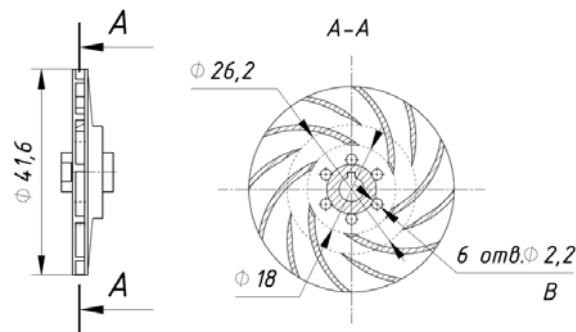


Fig. 3. Pump impeller:
 B – discharging holes

Рис. 3. Рабочее колесо насоса:
 B – разгрузочные отверстия

According to the calculations, the value of the acting axial thrust in an EPU of a similar design with an impeller without discharge holes is in the range from 1 to 8 N, depending on the pressure drop. According to the technical specifications for the electric motor, in order to ensure the required service life, the axial thrust should not exceed 8.7 N. In order to increase the service life of the bearing supports, we will consider ways to reduce the axial force without changing the design of the pump flow path and minimal changes in the impeller.

The influence of the position of the end of the impeller relative to the diffuser and the influence of the presence of discharging holes. One of the simplest ways to reduce the effect of axial force is to drill holes in the main impeller disc. Full unloading of the rotor will be achieved in the case $(P_B \cdot S_B) = (P_A \cdot S_A)$ [5; 6].

Taking into account the current design of the pump impeller shown in fig. 3, the total area of the discharging holes is 9 % of the area of the holes required to completely unload the rotor from the axial thrust. The position of the impeller relative to the spiral bend can affect the flow conditions of the working fluid in its vicinity. Each position of the impeller corresponds to a radial clearance X (remote element A, fig. 1), it affects the leakage through the front seal (q_1) and the rear seal (q_2), shown in fig. 2. In accordance with [6], any change in the gap in the seals or the nature of the movement in the sinuses causes an additional axial force due to the unbalanced part of the pressure diagram arising from the impeller geometry. Let

us check experimentally the pressure values from the rear side of the electric motor at different positions of the impeller relative to the spiral bend.

Experiment № 1. Study of the position of the end of the impeller relative to the diffuser; discharge holes are present. Setting up the experiment: the pressure on the pump impeller is investigated at various pressure heads. Pump configuration: the impeller has relief holes shown in fig. 3, tests were carried out with an electric motor DBE63-25-6.3 by measuring the pressure in the bearing area (on the back of the electric motor). The impeller is installed with different clearances X (0 mm and 0.4 mm, see fig. 1) relatively to the spiral bend. These clearances are obtained from the calculation of dimensional chains. Fig. 1 shows a fragment of the EPU used in the experiment with different clearance X. The assumption is tested that at different clearances different conditions of the flow of the power fluid in the EPU impeller are presented, and at X = 0.4 mm the pressure on the back side of the impeller will be greater will lead to increased axial thrust. During the experiment, the flow-pressure characteristics of the EPU were measured [7].

Experiment № 2. Investigation of the position of the end of the impeller relative to the diffuser, the discharge holes are closed. Setting up the experiment: similar to experiment № 1, except for the configuration of the impeller, since there are discharging holes in it. The experimental results are presented in tab. 2–4.

Table 2

Flow-pressure characteristics of EPU, pressure drop is 0.4 kgf/cm²

Parameter name	Atmospheric pressure				Pressure of 1.2 kgf/cm ²			
	Holes		No holes		Holes		No holes	
	X = 0	X = 0.4	X = 0	X = 0.4	X = 0	X = 0.4	X = 0	X = 0.4
Pressure from the back of the electric motor, kgf/cm ²	-0.15	-0.1	0.24	0.24	0.05	0.06	0.43	0.423
EPU inlet pressure, kgf/cm ²	-0.08	-0.05	-0.05	-0.05	0.13	0.13	0.14	0.129
EPU outlet pressure, kgf/cm ²	0.32	0.35	0.35	0.35	0.53	0.53	0.54	0.529
Heat transfer fluid consumption, cm ³ /s	0.32	0.35	0.35	0.35	0.53	0.53	0.54	0.529
Consumption current, A	>225	>225	228	>220	>225	>225	>228	>220
Heat transfer fluid temperature, °C	1.39	1.36	1.33	1.28	1.4	1.37	1.34	1.28

Table 3

Flow-pressure characteristics of EPU, pressure drop is 0.5 kgf/cm²

Parameter name	Atmospheric pressure				Pressure of 1.2 kgf/cm ²			
	Holes		No holes		Holes		No holes	
	X = 0	X = 0.4	X = 0	X = 0.4	X = 0	X = 0.4	X = 0	X = 0.4
Pressure from the back of the electric motor, kgf/cm ²	-0.12	-0.07	0.27	0.28	0.08	0.1	0.47	0.465
EPU inlet pressure, kgf/cm ²	-0.06	-0.03	-0.03	0.027	0.15	0.15	0.16	0.15
EPU outlet pressure, kgf/cm ²	0.44	0.47	0.47	0.473	0.65	0.65	0.66	0.65
Heat transfer fluid consumption, cm ³ /s	199	196	189	182	202	194	194	180
Consumption current, A	1.25	1.21	1.14	1.09	1.26	1.21	1.16	1.08
Heat transfer fluid temperature, °C	27.9	29.0	26.3	25.4	28.4	29.8	27.0	26.2

Flow-pressure characteristics of EPU, pressure drop is 0.6 kgf/cm²

Parameter name	Atmospheric pressure				Pressure of 1.2 kgf/cm ²			
	Holes		No holes		Holes		No holes	
	X = 0	X = 0.4	X = 0	X = 0.4	X = 0	X = 0.4	X = 0	X = 0.4
Pressure from the back of the electric motor, kgf/cm ²	-0.08	-0.03	0.33	0.346	0.12	0.14	0.52	0.527
EPU inlet pressure, kgf/cm ²	-0.03	0	-0.005	0.002	0.19	0.18	0.19	0.18
EPU outlet pressure, kgf/cm ²	0.57	0.6	0.595	0.602	0.79	0.78	0.79	0.78
Heat transfer fluid consumption, cm ³ /s	121	122	116	95	121	119	114	94
Consumption current, A	1.01	0.99	0.93	0.83	1.02	0.99	0.92	0.83
Heat transfer fluid temperature, °C	28.0	29.2	26.4	25.6	28.2	29.9	27.1	26.3

Let us compare the results obtained for different values of the clearance X and the presence or absence of relief holes. Comparison will be applied to the value of pressure from the rear side of the electric motor, since the axial force arises from the pressure difference on both sides of the impeller, and the value of the axial force itself is characterized by the integral of pressure.

Study of the influence of the number and shape of the impeller blades. According to [8], the number of impeller blades should be 6–7 in order to obtain a stable flow-pressure characteristic. In accordance with [9], the rational number of blades for a low-flow pump is 4–6. The pressure pulsations excited during the operation of the EPU cause pressure fluctuations in adjacent cavities, thereby affecting the direction, magnitude and nature of the axial force. It was found that the geometrical and operating parameters have a significant effect on the frequency spectrum and amplitude of pressure pulsations [9]. It is assumed that an increase in the number of blades leads to a more uniform distribution of speeds in the impeller, which will entail a decrease in pressure pulsations, which will cause a change in the nature of the movement of the liquid in the impeller. The task was to determine the effect of the number of blades on the axial thrust.

In this part of the experiment, additive technologies were used. They allowed to reduce test time due to the rapid production of various solutions. A printer with DLP printing technology was used. The principle of operation of which consists in gradual hardening along the sections of the part by illuminating the photopolymer with ultraviolet light. This technology made it possible to manufacture EPU impellers without using additional soldering operations, which positively affected the time spent on the production of experimental parts [10]. Of all the available printing technologies, this one is the most suitable because it allows the complex geometry of the impeller. The printing error is equal to the error of a milling machine, on which such impellers are usually manufactured. In addition, this technology does not require auxiliary elements for printing (support), which are necessary when using, for example, FDM technology, which decisively affects the quality of the resulting part. For further confidence in the results obtained using this technology, an

experiment was carried out. Measurements of flow-pressure characteristics and axial thrust were carried out for an impeller made of standard material (AMg6M) and an impeller of a similar design made of photopolymer, the results are presented in tab. 5.

It can be concluded that the impeller made of photopolymer shows flow-pressure characteristics lower than the impeller made of standard material, presumably due to the absence of sharp edges. However, we assume that this convergence is considered acceptable for a quick check of design solutions.

Experiment № 4. Investigation of the influence of the number of blades on the value of the axial force arising during the operation of the impeller in the EPU. With the help of the CAD - system, 3D models of EPU impellers were designed, presented below [11–15]. The shape of the blades was chosen on the basis of experimental experience, it provides the necessary blade frequency and allows you to obtain the flow-pressure characteristics presented in tab. 1. This result is the most suitable for the work of EPU. The subject of research in this work is the axial thrust arising from the functioning of the investigated impellers. The measurements were carried out using the setup shown in fig. 4, alternately in two types of enclosures shown in fig. 5. Vibration measuring information was obtained and analyzed on the electric motor DBE 63-25-6.3 with alternately installed impellers. Nominal parameters of EPU: the rotor speed of the electric motor during all tests was 5900 rpm. When registering vibration accelerations, the transducers were installed in accordance with fig. 5.

Registration of vibration acceleration signals was carried out using a set of means for multichannel recording of vibration parameters based on an LMS SCADAS Mobile measuring amplifier with the following recording parameters:

- 1) signal recording bandwidth – from 7 to 10240 Hz;
- 2) registration mode – continuous;
- 3) recording duration – 30 minutes;
- 4) sampling rate – 20480 Hz;
- 5) the sensor provides a three-axis measurement;
- 6) start mode – manual.

Signal processing was carried out using software LMS.Test.Xpress 5A (during signal recording) in order to

obtain the root mean square value (RMS) of vibration acceleration.

The cavity in which the impeller is located is filled with the power fluid LZ-TK-2. An axial force is created from the side of sensor 1. The electric motor is switched on. As the readings of the axial force on the sensor increase, it is gradually increased until it stops increasing or decreasing. When the force stops increasing, it means that the axial thrust from the sensor side is equal to the force from the impeller. The resulting value is the axial force acting from the impeller.

The axial thrust was measured under the following conditions:

- 1) the same flow path of the pump;
- 2) electric motor DBE 63-25-6.3;
- 3) the same position of the impellers relative to the spiral bend, discharging holes are present (in accordance with the calculation of dimensional chains $X = 0$). The choice is due to the result of experiment №1, according to which, at $X = 0$ and the presence of discharging holes, the pressure on the rear side of the electric motor decreased from 4 to 8 times;
- 4) power fluid LZ-TK-2.

Consider the options for the tested impellers.

16 blades, shortened in comparison with the ones of a standard impeller in fig. 2, axial thrust balancing discharging holes are present. Tab. 6, 7 show the test results of the impeller shown in fig. 6.

Impeller with 14 blades, which are shortened compared to the standard one, discharge holes for axial thrust compensation are present. Tab. 8–10 show the test results of the impeller shown in fig. 7.

Two tests were carried out:

- 1) discharge holes with a diameter of 2.2 mm;
- 2) discharge holes with a diameter of 3.2 mm.

After obtaining the results given in table 8, it was decided to widen the discharging holes in order to verify the calculations, according to which, with an increase of the discharging holes to a diameter of 3.2, the value of the axial thrust will decrease by 38 %.

Impeller with 14 straight blades. Tab. 11, 12 show the test results of the impeller shown in fig. 8.

Impeller with 14 long blades. Tab. 13, 14 show the test results of the impeller shown in fig. 9.

Tab. 15 shows the results of measuring the axial thrust in the impellers above.

Table 5

Flow-pressure characteristics of an AMg6M impeller and a photopolymer impeller of a similar design

Impeller material	Head (ΔP), kgf/cm ²	Flow rate (Q), m ³ /s	Rotational speed of the electric motor (n), rpm	Power fluid
AMg6M	0.61	110–150	5800	LZ-TK-2
Photopolymer	0.57	112	5800	LZ-TK-2

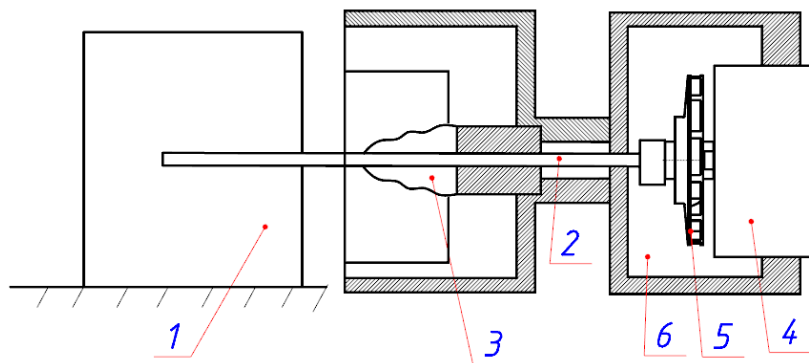


Fig. 4. Measurement circuitry:
1 – sensor; 2 – the rod; 3 – rubber gasket; 4 – motor; 5 – impeller;
6 – inner cavity with power fluid

Рис. 4. Схема измерения:
1 – датчик; 2 – шток; 3 – резиновое уплотнение; 4 – ЭД; 5 – рабочее колесо;
6 – внутренняя полость ЭНА, заполненная LZ-TK-2

Table 6

Test results, discharge holes \varnothing 2.2 mm

Pressure drop, kgf/cm ²	Consumption, cm ³ /s	Axial force, N (g)	Electric motor speed, n, rpm
0,4	189	2.8 (290)	5900

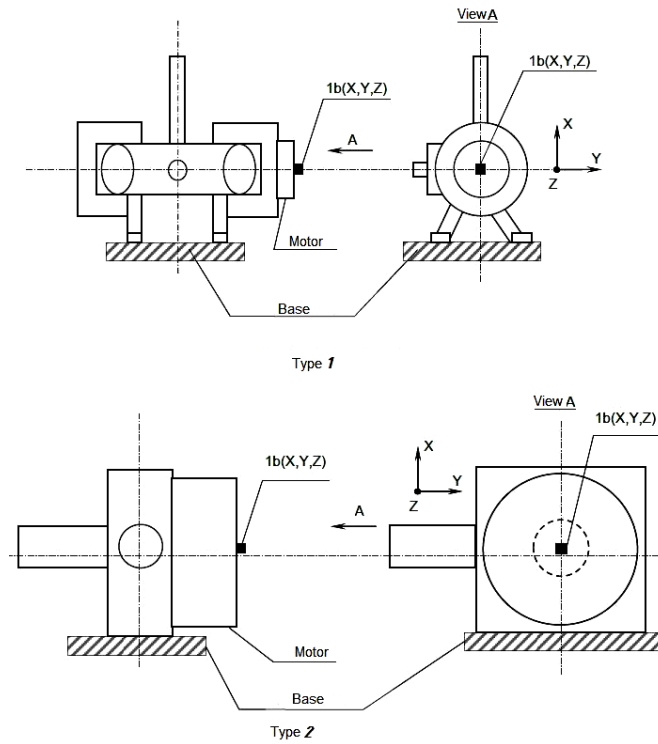


Fig. 5. Installation diagram of vibration transducers on the EPU electric motor

Рис. 5. Схема установки вибропреобразователей на ЭД ЭНА

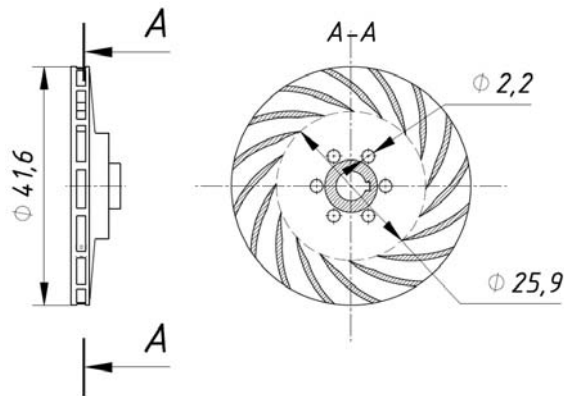


Fig. 6. Impeller with sixteen blades. The blades are shortened in comparison to the ones of a standard impeller

Рис. 6. Рабочее колесо с 16 лопатками, укороченными по сравнению со штатным

Table 7

RMS vibration acceleration of the impeller with 16 shortened blades

EPU type	Rotation speed, rpm	RMS by range 10–10240 Hz, m/s ²			RMS by range 10–3200 Hz, m/s ²			RMS by range 10-1000 Hz, m/s ²			Average RMS vibration acceleration, m/s ² (g)
		X	Y	Z	X	Y	Z	X	Y	Z	
Type 2	5900	1.79	1.73	3.16	1.30	0.77	1.32	0.26	0.34	0.14	0.27 (0.026)
Type 1		1.36	1.75	2.80	0.81	1.02	0.84	0.22	0.32	0.32	

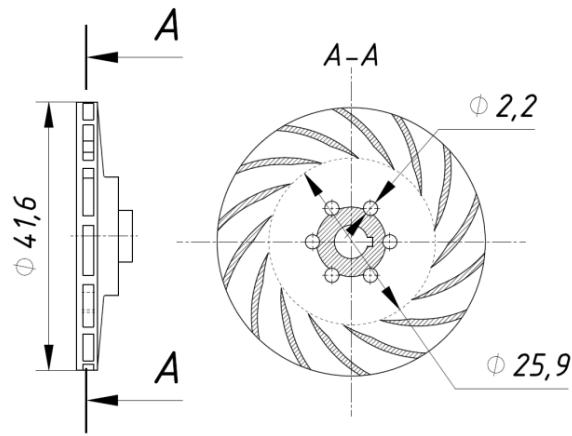


Fig. 7. An impeller with fourteen blades. The blades are shortened in comparison to the ones of a standard impeller

Рис. 7. Рабочее колесо с 14 лопатками, укороченными по сравнению со штатным

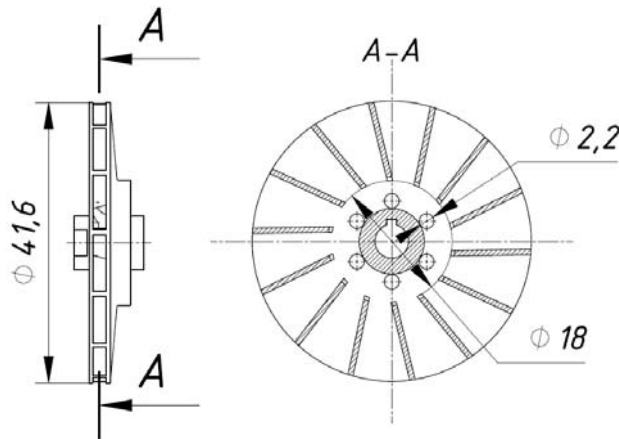


Fig. 8. Impeller with fourteen straight blades

Рис. 8. Рабочее колесо с 14 прямыми лопатками

Table 8

Test results, discharge holes $\text{Ø} 2.2 \text{ mm}$

Pressure drop, kgf/cm^2	Consumption, cm^3/s	Axial force, N (g)	Electric motor speed, n, rpm
0.4	189	1.66 (170)	5900

Table 9

RMS vibration acceleration of the impeller with 14 shortened blades

EPU type	Rotation speed, rpm	RMS by range 10–10240 Hz, m/s^2			RMS by range 10–3200 Hz, m/s^2			RMS by range 10–1000 Hz, m/s^2			Average RMS vibration acceleration, m/s^2 (g)
		X	Y	Z	X	Y	Z	X	Y	Z	
Type 2	5900	1.47	1.96	3.12	0.87	1.31	0.95	0.36	0.44	0.20	0.27 (0.026)
Type 1		1.85	2.43	2.93	1.01	1.51	0.74	0.23	0.31	0.27	

Table 10

Test results, discharge holes Ø 3.2 mm

Pressure drop, kgf/cm ²	Consumption, cm ³ /s	Axial force, N (g)	Electric motor speed, n, rpm
0.4	162	1.02 (105)	5900

Table 11

Test results, discharge holes Ø 2.2 mm

Pressure drop, kgf/cm ²	Consumption, cm ³ /s	Axial force, N (g)	Electric motor speed, n, rpm
0.4	227	2.69 (275)	5900

Table 12

RMS vibration acceleration of the impeller with 14 straight blades

EPU type	Rotation speed, rpm	RMS by range 10–10240 Hz, m/s ²			RMS by range 10–3200 Hz, m/s ²			RMS by range 10–1000 Hz, m/s ²			Average RMS vibration acceleration, m/s ² (g)
		X	Y	Z	X	Y	Z	X	Y	Z	
Type 2	5900	2.79	2.73	3.46	2.23	1.73	1.19	0.40	0.56	0.28	0.41 (0.042)

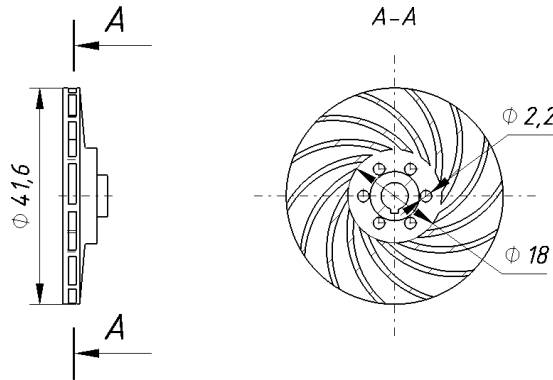


Fig. 9. Impeller with 14 long blades

Рис. 9. Рабочее колесо с 14 длинными лопатками

Table 13

Flow and pressure characteristics, axial thrust of impeller with 14 long blades, discharge holes Ø 2.2 mm

Pressure drop, kgf/cm ²	Consumption, cm ³ /s	Axial force, N (g)	Electric motor speed, n, rpm
0.42	210	> 2.69 (> 275)	5900

Table 14

RMS vibration acceleration of the impeller with 14 long blades

EPU type	Rotation speed, rpm	RMS by range 10–10240 Hz, m/s ²			RMS by range 10–3200 Hz, m/s ²			RMS by range 10–1000 Hz, m/s ²			Average RMS vibration acceleration, m/s ² (g)
		X	Y	Z	X	Y	Z	X	Y	Z	
Type 2	5900	3.73	4.43	3.16	2.97	3.14	1.63	0.42	0.51	0.30	0.41 (0.042)

Results of measuring the axial thrust in impellers with different blades

№	Impeller type	Axial thrust, N	Average RMS vibration acceleration, m/s ² (g)
1	16 short blades	2.84	0.27 (0.026)
2	14 short blades	1.66/1.02	0.30 (0.029)
3	14 straight blades	2.69	0.41 (0.042)
4	14 long blades	> 2.69	0.41 (0.042)

Conclusion. With the same clearance and only from the presence of discharge holes, the value of the pressure acting from the rear side of the electric motor decreased approximately 2–3 times in the absence of pressure and up to four times in the presence of pressure of 1.2 kgf/cm². The introduction of discharging holes for reducing the magnitude of the axial force acting in the electric pump unit is a widespread measure due to its simplicity and efficiency, which is confirmed by this experiment.

There was no change in the magnitude of the pressure on the rear side of the electric motor when the clearance X was changed from 0 to 0.4. However, there is a small change in flow rate (from 7 to 21 cm³/s) when the clearance X changes from 0 to 0.4 in the case of holes present. A similar phenomenon was not detected in the case of the absence of discharge holes.

When comparing the case with the presence of discharge holes and a clearance of X = 0 (case 1) with the case of the absence of discharge holes and a clearance of X = 0.4 (case 2), it was revealed that the pressure on the back of the electric motor decreased from 4 to 8 times in case 1 compared with case 2 in the presence of pressure of 1.2 kgf/cm². In the absence of a pressure of 1.2 kgf/cm², the pressure from the rear side of the electric motor decreased from 1.5 to 4 times.

The size of the discharge holes affects the amount of axial force that occurs when the impeller operates. With an increase in the diameter of the discharge holes by 45 %, the magnitude of the axial force decreased by 62 %. A further increase in the diameter of the discharge openings is considered impractical due to the increase in head losses.

According to the results of the analysis of vibration measurement information, for impellers with a different number of blades of the selected shape, the amplitudes of peaks above 1000 Hz prevail in the vibration acceleration spectra. This value is the most suitable for EPU operation.

With an increase in the number of blades from 14 to 16, the axial thrust increased by 4 %.

When changing the shape of the blade to a straight line (variant 3 of tab. 15), the value of the axial force increased by 62 %.

According to the results of the analysis of vibration measurement information for impellers with a different number of blades of the selected shape, the amplitudes of peaks above 1000 Hz prevail in the vibration acceleration spectra. This result is most suitable for the work of EPU.

The vibration acceleration spectra also show a significant predominance of the peak amplitudes in the range above 1000 Hz. The minimum parameters of the RMS vibration acceleration module are observed for the impeller with 16 short blades.

The use of additive DLP printing technology in this study significantly accelerated the testing process. Impellers made of photopolymer have flow-pressure characteristics close to those of impellers made of standard material.

References

- Ley W., Wittman K., Hallmann W. Handbook of Space Technology, 2009, 884 p.
- Sarafin T. P, Larson W. J. Spacecraft structures and mechanisms. From Concept to Launch, 2007, 850 p.
- Lomakin A. A. *Tsentrobeznyye i osevye nasosy* [Centrifugal and axial pumps]. Moscow, Mashinostroenie Publ., 1996, 364 p.
- Zimnitskiy V. A. et al. *Lopastnye nasosy* [Vane pumps]. Leningrad, Mashinostroenie Publ., 1986, 334 p.
- Perevoshchikov S. I. *Konstruktsiya tsentrobeznykh nasosov (obshchie svedeniya)* [The design of centrifugal pumps (general information)]. Tyumen, Tsogu Publ., 2013, 228 p.
- Malyushenko V. V., Mikhaylov A. K. *Energeticheskie nasosy* [Energy pumps]. Moscow, Energoizdat Publ., 1981, 200 p.
- Yarementko O. V. *Ispytaniya nasosov* [Pump Testing]. Moscow, Mashinostroenie Publ., 1976, 225 p.
- Mikhaylov A. K., Malyushenko V. V. *Lopastnye nasosy. Teoriya, raschet i konstruirovaniye*. [Vane pumps. Theory, calculation and construction]. Moscow, Mashinostroenie Publ., 1977, 288 p.
- Kraev M. V., Lukin V. A., Ovsyannikov B. V. *Maloraskhodnye nasosy aviatsionnykh i kosmicheskikh sistem* [Low-flow pumps of aviation and space systems]. Moscow, Mashinostroenie Publ., 1985, 128 p.
- Zlenko M. A., Nagaytsev M. V., Dovbysh V. M. *Additivnye tekhnologii v mashinostroenii. Posobie dlya inzhenerov* [Additive technologies in mechanical engineering. A manual for engineers]. Moscow, NAMI Publ., 2015, 220 p.
- Baybakov O. V. *Primenenie EVM v raschetakh protochnoy polosti lopastnykh gidromashin* [The use of computers in the calculations of the flowing cavity of paddle hydraulic machines]. Moscow, MG TU im. N. E. Bauman Publ., 1982, 65 p.

12. Branshteyn L. Ya. *Spravochnik konstruktora gidroturbin* [Hydroturbine Designer Reference]. Moscow, Mashinostroenie Publ., 1971, 304 p.

13. Sazonov Yu. A., Mulyenko V. V., Balaka A. Yu. [Computer modeling and development of a methodology for designing dynamic pumps and machines]. *Territoriya neftegaz*. 2011, No. 10, P. 34–36 (In Russ.).

14. Karelin V. Ya. *Kavitatsionnye yavleniya v tsentrobеzhnykh i osevykh nasosakh* [Cavitation phenomena in centrifugal and axial pumps]. Moscow, Mashinostroenie Publ., 1976, 325 p.

15. Loytsyanskiy L. G. *Mekhanika zhidkosti i gaza* [Mechanics of fluid and gas]. Moscow, Drofa Publ., 2003, 840 p.

Библиографические ссылки

1. Ley W., Wittman K., Hallmann W. *Handbook of Space Technology*, 2009. 884 p.

2. Sarafin T. P., Larson W. J. *Spacecraft structures and mechanisms. From Concept to Launch*, 2007. 850 p.

3. Ломакин А. А. Центробежные и осевые насосы. М. : Машиностроение, 1996. 364 с.

4. Лопастные насосы : справочник / В. А. Зимницкий и др. Л. : Машиностроение, 1986. 334 с.

5. Перевошиков С. И. Конструкция центробежных насосов (общие сведения). Тюмень : ТюмГНГУ, 2013. 228 с.

6. Малюшенко В. В., Михайлов А. К. Энергетические насосы. М. : Энергоиздат, 1981. 200 с.

7. Яременко О. В. Испытания насосов. М. : Машиностроение, 1976. 225 с.

8. Михайлов А. К., Малюшенко В. В. Лопастные насосы. Теория, расчет и конструирование. М. : Машиностроение, 1977. 288 с.

9. Краев М. В., Лукин В. А., Овсянников Б. В. Малорасходные насосы авиационных и космических систем. М. : Машиностроение, 1985. 128 с.

10. Зленко М. А., Нагайцев М. В., Довбыш В. М. Аддитивные технологии в машиностроении. М. : НАМИ, 2015. 220 с.

11. Байбаков О. В. Применение ЭВМ в расчетах проточной полости лопастных гидромашин. М. : МГТУ им. Н.Э. Баумана, 1982. 65 с.

12. Бранштейн Л. Я. Справочник конструктора гидротурбин. М. : Машиностроение, 1971. 304 с.

13. Сазонов Ю. А., Муленко В. В., Балака А. Ю. Компьютерное моделирование и развитие методологии конструирования динамических насосов и машин // *Территория нефтегаз*. 2011. № 10. С. 34–36.

14. Карелин В. Я. Кавитационные явления в центробежных и осевых насосах. М. : Машиностроение, 1976. 325 с.

15. Лойцянский Л. Г. *Механика жидкости и газа*. М. : Дрофа, 2003. 840 с.

© Kuznetsova Z. A., Sinichenko M. I., Kuznetsov A. D., Kleshnina I. A., Sin'kovskiy F. K., 2020

Kuznetsova Zoya Alekseevna – category 3 design engineer; JSC Academician M. F. Reshetnev Information Satellite Systems. E-mail: u-z-a@yandex.ru.

Sinichenko Mikhail Ivanovich – head of department; JSC Academician M. F. Reshetnev Information Satellite Systems. E-mail: smi320@iss-reshetnev.ru.

Kuznetsov Artem Dmitrievich – category 2 design engineer; JSC Academician M. F. Reshetnev Information Satellite Systems. E-mail: tember63@mail.ru.

Kleshnina Irina Aleksandrovna – category 3 design engineer, JSC Academician M. F. Reshetnev Information Satellite Systems. E-mail: kleshninaia@iss-reshetnev.ru.

Sin'kovskiy Fedor Konstantinovich – Deputy director of the Industrial Center for Large-Sized Foldable Mechanical Structures; JSC Academician M. F. Reshetnev Information Satellite Systems. E-mail: sfk@iss-reshetnev.ru.

Кузнецова Зоя Алексеевна – инженер-конструктор третьей категории; АО «Информационные спутниковые системы имени академика М. Ф. Решетнева». E-mail: u-z-a@yandex.ru.

Синиченко Михаил Иванович – начальник сектора; АО «Информационные спутниковые системы» имени академика М. Ф. Решетнева». E-mail: smi320@iss-reshetnev.ru.

Кузнецов Артем Дмитриевич – инженер-конструктор второй категории; АО «Информационные спутниковые системы» имени академика М. Ф. Решетнева». E-mail: tember63@mail.ru.

Клешнина Ирина Александровна – инженер-конструктор третьей категории; АО «Информационные спутниковые системы» имени академика М. Ф. Решетнева». E-mail: kleshninaia@iss-reshetnev.ru.

Синьковский Федор Константинович – заместитель директора – главный конструктор отраслевого центра крупногабаритных трансформируемых механических систем; АО «Информационные спутниковые системы» имени академика М. Ф. Решетнева». E-mail: sfk@iss-reshetnev.ru.
